Applied Spectroscopy Reviews

ISSN: 0570-4928 (Print) 1520-569X (Online) Journal homepage: https://www.tandfonline.com/loi/laps20

Near-Infrared spectroscopy and hyperspectral imaging for non-destructive quality assessment of cereal grains

Nicola Caporaso, Martin B. Whitworth & Ian D. Fisk

To cite this article: Nicola Caporaso, Martin B. Whitworth & Ian D. Fisk (2018) Near-Infrared spectroscopy and hyperspectral imaging for non-destructive quality assessment of cereal grains, Applied Spectroscopy Reviews, 53:8, 667-687, DOI: 10.1080/05704928.2018.1425214

To link to this article: https://doi.org/10.1080/05704928.2018.1425214

Published online: 30 Jan 2018.

APPLIED SPECTROSCOPY REVIEWS
2018, VOL. 53, NO. 8, 667–687
https://doi.org/10.1080/05704928.2018.1425214

Taylor & Francis
Taylor & Francis Group

Near-Infrared spectroscopy and hyperspectral imaging for non-destructive quality assessment of cereal grains

Nicola Caporaso[a,b], Martin B. Whitworth[b], and Ian D. Fisk[a]

[a]Division of Food Sciences, School of Biosciences, University of Nottingham, Leicestershire, UK; [b]Campden BRI, Department of Primary Production & Processing, Chipping Campden, Gloucestershire, UK

ABSTRACT

Hyperspectral imaging (HSI) combines spectroscopy and imaging, providing information about the chemical properties of a material and their spatial distribution. It represents an advance of traditional Near-Infrared (NIR) spectroscopy. The present work reviews the most recent applications of NIR spectroscopy for cereal grain evaluation, then focuses on the use of HSI in this field. The progress of research from ground material to whole grains and single kernels is detailed. The potential of NIR-based methods to predict protein content, sprout damage and α-amylase activity in wheat and barley is shown, in addition to assessment of quality parameters in other cereals such as rice, maize and oats, and the estimation of fungal infection. This analytical technique also offers the possibility to rapidly classify grains based on properties such as variety, geographical origin, kernel hardness, etc. Further applications of HSI are expected in the near future, for its potential for rapid single-kernel analysis.

KEYWORDS

Hyperspectral chemical imaging; NIR spectral imaging; cereal quality; single grains analysis; non-destructive analysis; wheat

1. Introduction

Near-infrared (NIR) spectroscopy is widely applied in food science and technology research, and is one of the most common analytical techniques in the sector due to its low costs, rapidity and non-destructive nature (1).

Hyperspectral imaging (HSI) combines the advantages of spectroscopy, i.e., the rapidity and non-destructive nature, with the possibility of analyzing the spatial distribution of quality parameters of foods, by using imaging technology. An illustration of an HSI system working in the "push-broom" mode is shown in Figure 1, while Figure 2 shows an example of HSI hypercube and the steps involved in the prediction.

HSI was originally developed for remote sensing applications, and has since been applied in many fields, e.g. remote sensing, astronomy, pharmaceuticals, agriculture and

CONTACT Nicola Caporaso nicola.caporaso@nottingham.ac.uk Division of Food Sciences, Sutton Bonington Campus, University of Nottingham, Sutton Bonington, Leicestershire LE12 5RD, UK; Ian D. Fisk ian.fisk@nottingham.ac.uk Division of Food Sciences, Sutton Bonington Campus, University of Nottingham, Sutton Bonington, Leicestershire LE12 5RD, UK.

Color versions of one or more of the figures in the article can be found online at www.tandfonline.com/laps.

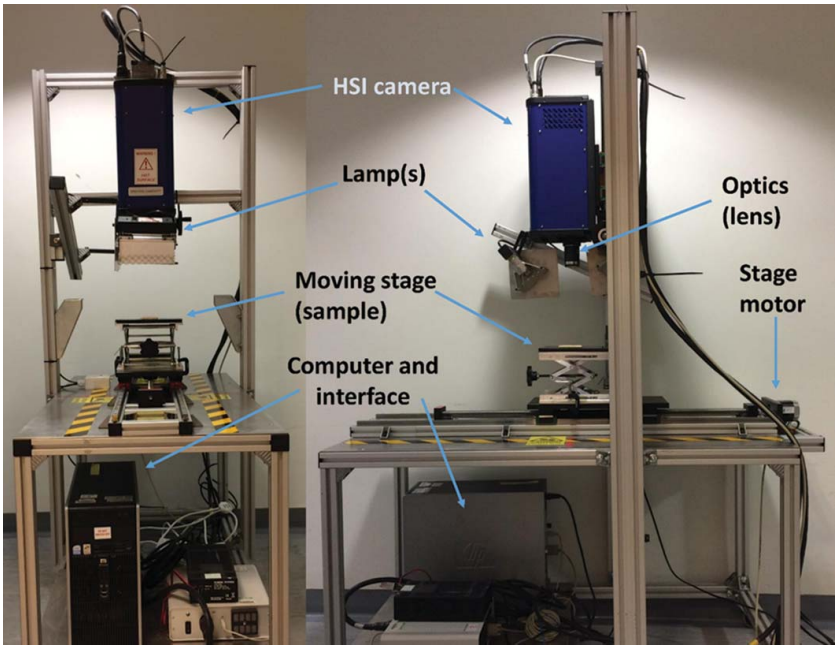

Figure 1. Example of a hyperspectral imaging system for acquiring data in the "push-broom" mode.

medicine (2). The information recorded in HSI represents three-dimensional data which contains the spatial information of the image and the spectral data, and is called a "hypercube." The general principle of hyperspectral imaging, the different types of hardware configurations and settings available, as well as food applications outside cereal grains can be found elsewhere (3, 4). Other sources gave reviews focusing on food quality and safety (2, 5), or described the steps involved in the data processing and extraction of useful information from the hypercube (6). Thus, these aspects are not detailed in the current paper. Other reviews reported on the application of HSI in food safety inspection and control (7), or for fruit and vegetable quality assessment (8). These works demonstrate the potential of the HSI technology for a wide variety of food products and quality parameters, while the present review focuses on the most recent applications of NIR spectroscopy and HSI for the evaluation of cereal grains, particularly with works dealing with the assessment of variability at single kernel level.

Cereals are a staple food worldwide; wheat, rice, and maize represent the most important agricultural crops and provide more than half of the world's dietary calorific intake. The quality of food products is strictly dependent on the quality of the raw ingredients used. Therefore, assessing their composition, purity and physico-chemical characteristics is of interest for the food industry, breeders and farmers, and for the scientific community serving these industries.

This review describes the developments of NIR-based methods for quality evaluation of cereal grains, in particular for whole kernels and single kernel applications, and the most promising applications of HSI for these commodities are described, with an emphasis on the prediction of grain composition. Spectral pre-processing and chemometrics, in particular multivariate statistics, are of fundamental importance to obtain reliable HSI prediction models. Spectral pre-processing methods have been developed to correct for light scattering and

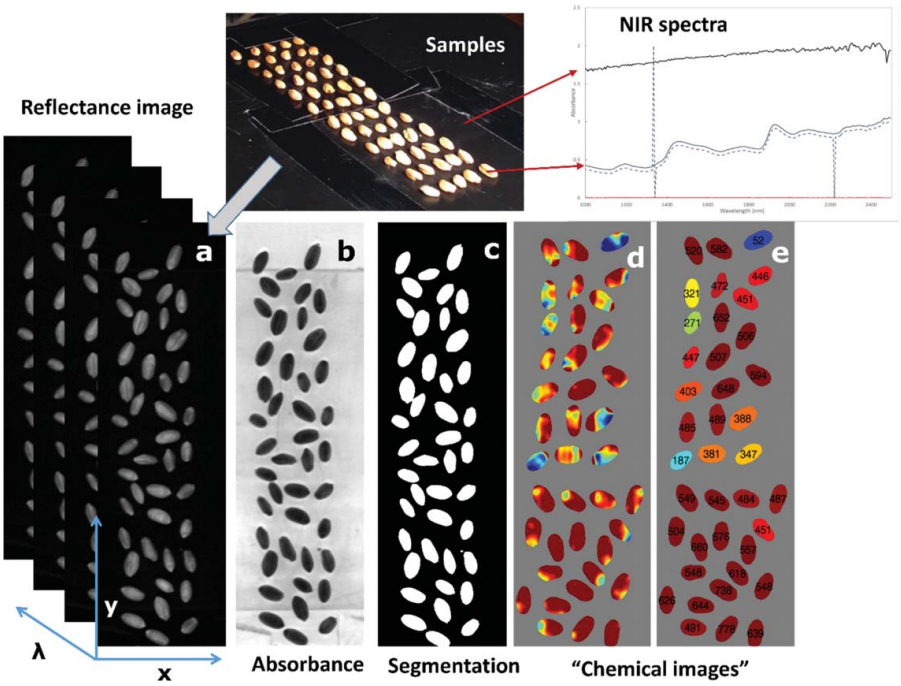

Figure 2. Example of hyperspectral images ("hypercubes") obtained by HSI, showing wheat kernels. The samples are presented on the acquisition stage, with indication of the reflectance spectrum at one pixel belonging to the black plastic stage (background), and one pixel belonging to a wheat kernel. The dotted line indicates the spectrum before the spike correction. (a) Reflectance image at a particular wavelength, showing the three-dimensional structure of the hypercube. (b) Absorbance image, for the same image, and (c) segmentation necessary to remove the background and select the region of interest for further analyses. (d) Application of a quantitative prediction at a single pixel level, obtaining the so-called "chemical image" (colors indicate different concentrations of a compound); (e) calculation of the average content of a compound or property on a single kernel level (numbers indicate the predicted Hagberg Falling Number, as in Caporaso et al. (44)).

other spectral variation unrelated to the chemical composition. HSI involves considerably higher requirements than NIRS in terms of data processing, due to the larger dataset. Recent reviews have been published on these aspects (9, 10).

The aim of our article is to give an overview of the latest development of NIR spectroscopy-based techniques applied to cereal grain evaluation, by then focusing on the advantages and potential of HSI for qualitative (classification) and quantitative prediction of grain properties, in particular chemical composition and novel applications.

2. Latest applications of NIR spectroscopy for wheat quality evaluation

Among the quality parameters considered for wheat, physical traits, moisture content, kernel hardness, protein content and falling number are the most important ones. The first applications of (NIR) spectroscopy for non-destructive protein analysis of cereals started decades ago (11, 12), and nowadays NIR spectroscopy is a well-recognized technique in the wheat and cereal-processing industry for routine quality assessment. Traditional applications of NIR spectroscopy for cereals used ground wheat (13). However, it was

demonstrated that reliable prediction of wheat composition is possible using NIR directly on the whole kernels, which represented a great advance with benefits in terms of sample preparation, cost, and applicability (14). NIR spectroscopy has been applied to predict some major constituents of grains such as moisture, protein, and lipids. It has demonstrated good performance so that in several cases, it is preferred over traditional wet chemistry methods for routine analysis, and has been successfully applied by the industry for decades, including on-line (15).

The use of ground material removes the information related to the natural variability of individual kernels within the batch, as it implies measurement of an average. Grinding gives a uniform material on the spectrometer window, therefore better predictions are usually obtained compared to whole kernel measurement, but grinding is time-consuming and it represents a limitation when large numbers of samples need to be scanned. After the demonstration of whole-kernel NIR predictions, further advance for grain analysis was represented by the demonstration that NIR spectroscopy is able to scan individual kernels instead of bulk. Delwiche (16) was one of the first authors that successfully applied NIR spectroscopy for the analysis of protein content on a single kernel basis, and several other properties were studied afterward. For example, single kernel NIR spectroscopy has been also applied for European wheats belonging to different classes and protein grades. The authors studied single seed protein, vitreousness, density, and hardness index in the NIR region in transmission mode, and obtained a very good calibration, particularly for hardness (17).

NIR was also applied to individual wheat kernels for variety identification in breeding programmes, showing potential for other crop breeding programmes (18). However, the major difficulty of variety identification comes from the similarity of wheat NIR spectra, any subtle spectral differences between different varieties are normally masked by intrinsic variation between individual grains.

Protein content in wheat has been a major target for NIR spectroscopists, for bulk and single kernel applications. For example, NIR reflectance spectroscopy has been applied to assess protein variability in single wheat kernels from four USA wheat classes, by using >300 samples and scanning 10 individual kernels for each in the spectral region 1100–2498 nm (19). Multivariate statistical models were constructed using Partial Least Squares (PLS) analysis or multiple linear regression (MLR) models. The protein content on single kernels ranged from 6 to 20% (12% moisture basis) in hard red winter wheats. The author also tested the possibility of using a limited region of the NIR spectrum, and reported the performances of the regions considered, 1100–1504 nm being the most appropriate. Both PLS and MLR models gave satisfactory results ($R^2 = 0.90–0.97$), with a slightly better performance when using PLS. In a further work, it was demonstrated that protein content in wheat may be estimated by single kernel NIR reflectance spectra at a performance equivalent to conventional bulk kernel NIR instrumentation (20).

2.1. Quantitative prediction for other cereals

Most of the scientific literature focuses on the economically relevant cereals for assessing quality parameters of cereals by NIR spectroscopy. Some papers have reported the application of NIRS for quality evaluation of other cereal grains, such as barley, oats, and triticale. Reflectance spectroscopy has been applied to whole barley grains to study the variation in moisture and nitrogen content (21). The calibration for total nitrogen was less accurate than

for moisture, and the influence of genotypes was reported. In particular, accuracy was higher when calibrations were developed for individual varieties.

Other authors reported protein prediction in barley and malt by NIR spectroscopy using PLS and MLS, under the spectral range 1100–2500 nm (22). The calibration built using MLR had a prediction error of 0.15 and 0.17%, for barley and malt, respectively. PLS regression gave a slightly higher standard error of prediction (SEP) of 0.22 and 0.27%, respectively.

The prediction ability of NIR on single kernels of barley for protein content quantification was also reported by Fox et al. (23). A total of 160 kernels with protein range 7.3–16.6% were used for the calibration model, and 20 as a validation set, obtaining $R^2 = 0.90$ for the calibration. Then, a commercial malting variety was used to scan 4,000 kernels, grouped according to their protein content. A wide variability of protein content in individual barley grains was reported, as within the same batch and variety, protein content ranged between 5.0 and 14.5%.

Malted barley was studied by Tarr et al. (24) to monitor the malting process by Raman and FTIR spectroscopy. Whole barley grains were scanned before and after the malting process using increasing germination times (2, 3, 4, and 5 days). Other parameters were tracked during the malting process, namely friability, β-glucan, wort viscosity and malt extract, as well as soluble nitrogen, free amino nitrogen, and diastase.

Recently, Han et al. (25) demonstrated that good prediction could be achieved for total phenolics and free p-coumaric acid content in barley grains using NIR spectroscopy. The authors used 130 barley genotypes and acquired reflectance spectra in the region 1100–2500 nm on the ground material, to build prediction models by PLS and least squares support vector machine (LS-SVM). For both compounds, the models had R^2 values above 0.93, for both calibration and prediction datasets.

Triticale, a hybrid of wheat and rye, is cultivated mainly for feed purposes, and has also been applied for baking and as a source of biofuel. Fontaine et al. (26) developed NIR calibrations to predict protein, moisture and essential amino acids in several cereals including triticale. 122 ground samples were scanned by reflectance NIR (1100–2500 nm), and all the prediction models had generally good performances, with the protein model for triticale showing $R^2 = 0.98$ and SECV = 0.235% (range 8.49–14.5%). A further advance for NIR spectroscopy studies of triticale quality was reported by Manley et al. (27), who developed a calibration model for whole or ground kernels, in the region 1900–2500 nm. Seven cultivars from two harvest years were sampled, obtaining a total of 195 samples. Protein and ash content, kernel hardness and SDS sedimentation were determined by reference methods. The most accurate calibration for protein content was obtained from spectra pre-processed using first derivative and normalization treatments. Differences in the prediction ability between whole and ground triticale were found, with SEC of 0.72 and 0.50%, respectively. As expected, prediction of moisture content improved using ground samples, while the best prediction was obtained from whole kernels for SDS sedimentation.

Other authors (28) scanned whole triticale kernels as bulk using transmittance NIR spectroscopy in the range 850–1050 nm, and applied a nonlinear calibration based on an Artificial Neural Network (ANN) previously built for wheat. A poorer calibration (protein SEP = 0.38%) was reported using this approach, compared to a dedicated triticale calibration, which had standard error of prediction of 0.29 and 0.30% for moisture and protein content, respectively.

Many other examples of conventional NIR spectroscopy applied to cereal grains can be found in the literature, especially for bulk analysis of ground material. However, this review

will focus on HSI and the additional advantages offered by this technology, reporting on the latest applications for grains.

3. The use of HSI for cereal grains evaluation

The majority of research papers reporting HSI applications to whole grain focus on classification methods, e.g. to discriminate extraneous material, or to assess differences within the batch, while more limited research has been carried out for quantification purposes. For example, a recent paper applied HSI for the classification of oat and groat kernels, which was suggested to be applicable at industrial level for the rapid measurement of the amount of hull-less oat kernels, this being one of the key quality parameters in this commodity (29). The authors used a HSI system working in the NIR range 1000–1700 nm and applied PLS Discriminant Analysis (PLS-DA) to discriminate between oat and groat samples. The classification model had accuracy above 99% for both classes. The following three wavelengths were the most important bands according to the variable importance in projection (VIP) scores: 1132, 1195, and 1608 nm. Using a prediction model based on these three spectral bands only, 97.1% and 99.0% correct classification rates were obtained on groat and oat, respectively (29).

Several authors highlighted the potential of HSI over simple NIR spectroscopy for the analysis of intact grains, but the use of HSI implies further data processing and the removal of spectral variation which is unrelated to the chemical composition. Manley et al. (30) reported on the influence of grain topography, i.e., shape and texture, when investigating the viability of whole wheat, barley and sorghum kernels. Kernel curvature was shown to be the major cause of variation for barley, wheat, and sorghum. Non-uniform lighting caused by sample curvature, kernel topography, and surface roughness influenced the spectra by altering reflection and scattering. Principal Component Analysis (PCA) showed that the first PCs were due to the nonuniformity of illumination and grain topography, in particular variations at the edges of the wheat kernels, as well as other physical factors such as the sample height, shape or surface texture. Some influence of the seed coat (or hull) texture in wheat, barley, and sorghum was also reported. Several physical phenomena contribute to the apparent light scattering effects, as the additive and multiplicative scatter effects may be caused by differences in kernel size, structure, and presentation angle (31). For these reasons, spectral treatment using appropriate mathematical algorithms is necessary to remove unwanted physical interferences. An overview of spectral pre-processing techniques is given by Rinnan et al. (32).

One potential area of application for HSI is the detection of extraneous material in food or feed products. HSI is especially suited for grains or solid granular material, as once a proper classification model is built, automatic recognition of different objects can be done by attributing each pixel to a particular class. An example of this approach was reported for the detection of impurities in wheat by HSI in the NIR range 1000–1600 nm (33). Different types of impurities were considered, i.e., the presence of other seeds such as barley, canola, maize, broken wheat kernels, wild oats, stones, and animal excreta. Classification models were constructed using the Naive Bayes (NB), Support Vector Machine (SVM), and *k*-nearest neighbours (k-NN) classifiers, which are machine learning techniques, and each non-wheat material was classified against wheat. A total of 4,800 individual sample particles, i.e., 300 particles/kernels × 16 sample types, were imaged. Among the foreign material, canola was most accurately classified while oats were the least accurately classified from wheat. When all the foreign materials were considered together, k-NN classification technique gave the best score, i.e., 90.1% accuracy,

with SNV as the best performing pre-treatment. k-NN also performed well for dockage discrimination (91.7% accuracy), and for animal excreta (99.9%).

Differentiation can be also made within the same type of grain, e.g., wheat, but aiming to classify for different varieties, types or classes, that might have different market price or grade. HSI was applied to differentiate Canadian wheats into eight classes (Canada Western Red Spring, Canada Prairie Spring Red, Canada Western Extra Strong, etc.) (34). Reflectance spectra were acquired in the NIR region 960–1700 nm using an area array. Eight wheat classes from Canadian wheats were sampled and conditioned at 11% moisture. Approximately 50 grams of wheat kernels were placed in Petri dishes. Artificial Neural Network (ANN), Linear Discriminant Analysis (LDA), and Quadratic Discriminant Analysis (QDA) were used for classification. This approach demonstrated accuracies ranging from 86 to 100% for validation, depending upon the statistical model applied and the wheat class. The authors proposed further studies involving samples at different moisture contents, and to improve the robustness of the classification models by using a wider range of samples from different locations.

Physical-related properties of grains have been also successfully applied based on HSI. Prediction of vitreousness in durum wheat kernels by HSI was reported using the spectral range 650–1100 nm and visual inspection as the reference method (35). A PLS-factorial discriminant analysis (FDA) model was used to classify kernels into three classes, showing classification rate up to 94%. Similar studies were carried out on Canadian wheats, which were scanned by a hyperspectral imaging system operating in the region 950–2500 nm to differentiate wheats into vitreous, starchy, and bleached kernels (36).

Very limited research has been reported so far for quantitative prediction models by HSI for cereal grains. HSI offers the great advantage to predict single grains even at relatively high throughput, so that grains with different composition can be rapidly evaluated by scanning multiple kernels per time. Recently, Caporaso et al. (37) applied HSI in the full NIR range (1000–2500 nm) to build calibration models based on PLS regression for protein content in single wheat kernels. Over 180 wheat batches were sourced from several locations, mainly within the UK, and individual kernels were taken from each batch, building prediction models on more than 3,200 kernels scanned on both sides. The comprehensive model including samples of hard and soft wheats had $R_c^2 = 0.82$ and $R_v^2 = 0.82$. The prediction error was 0.86% and 0.94% for the calibration and validation datasets, respectively. It was also shown that using the averaged spectra from each batch led to lower prediction error, but the method proposed allows rapid prediction of single kernel protein, which can be of interest for rapid screening in breeding programmes and for the industry. The application of calibration at the single pixel level was also shown to be effective in visualization of protein content distribution within single kernels. In addition, the authors simulated the use of lower cost detectors, working in the range 1000–1700 nm, which led to slightly lower prediction performance and higher prediction error, the best model showing RMSEP = 1.13%. The potential of predicting kernel weight using the HSI spectra was also reported.

4. HSI for sprouting detection, α-amylase activity, and β-glucan content

Enzymatic activity in cereal grains is related to germination and sprouting. Thus, it is of paramount importance for their relevance in malting during the brewing process and for adverse effects on bread-making quality of flour. α-Amylase is the most relevant enzyme for

wheat, barley, and other cereals (38). The problem of pre-harvest sprouting and late maturity amylase problems has been reviewed elsewhere (39).

A study by HSI assessed the changes in pre-germinated and germinated wheat kernels using an indium gallium arsenide (InGaAs) focal plane array detection system over the region 1000–1700 nm (40). Six wheat varieties were germinated from 3 to 48 h, and freeze-dried. No reference analyses were performed but the germination rate was assessed visually. A classification was performed according to the level of sprouting and there was an indication that sprouting level strongly depends on genotype, as the six varieties considered had different behaviors regarding germination response to moisture exposure.

HSI has been investigated to understand whether it is possible to estimate α-amylase activity in wheat, as visual methods are not always successful for this purpose (41–43). Xing et al. (41) applied HSI for the prediction of α-amylase activity in two Canadian wheat classes, a soft and a durum variety. The spectral region used was 1255–2300 nm, with 7 nm increments. PCA and PLS regression were used to set up a calibration model, using the spatial region belonging to the germ only. This was done as the statistical analysis indicated that the highest variability was localized in the germ region. The creation of a single calibration model for the two wheat classes was not possible, due to the different level of translucency and distribution of amylase activity. The individual wavelengths that were calculated as the most important predictors were: 1397, 1634, 1874, 2076 and 2228 nm for Canada Western Red Spring, and 1347, 1410, 1627, 1721, 2064 and 2159 nm for Canada Western Amber Durum. Nevertheless, the best prediction was obtained when using the full spectra. Relatively low values of R^2 of 0.54 and 0.73 were obtained for the two wheat classes, respectively. However, this could be sufficient for classification purposes, as the authors reported accuracy of discriminant analysis up to 94% for high α-amylase content and 88% for low level samples.

The same research group applied the visible region of the spectra (400–1000 nm) for similar purposes (42). The size at the ends of the kernels is a visual parameter that could theoretically be helpful in detecting pre-harvest germination in wheat, due to the swelling of the embryo during germination. This has been shown to be potentially detectable by HSI. Parameters such as the area ratio of the germ end to brush end of a kernel, or the ratio between absorbance at 878 and 728 nm were suggested as possible indicators of sound and sprouted kernels. However, the level of misclassified kernels was high, with approximately 65% of the sprouted kernels misclassified as sound. PCA allowed better classification accuracy (88%), while even more promising classification was obtained combining the two calculations in a single model, which gave 100% and 97% accuracy for sound and sprouted kernels, respectively (42).

Xing et al. (43) applied HSI in the NIR region (1000–2500 nm) to evaluate individual Canadian Western Red Spring wheat kernels. Two sets of 144 and 120 wheat kernels were artificially sprouted or allowed to germinate in the field. The results from HSI were compared to those obtained by an α-amylase activity reference measurement, and a PLS calibration model was built. Spectral intensities across the entire wavelength region were directly related to the enzymatic activity. The performances of SWIR HSI and traditional Fourier Transform NIR (FT-NIR) instruments were also assessed, the first method resulting in significantly better performance. Best results were achieved with a Savitzky–Golay second derivative treatment which allowed clustering samples according to their enzyme levels, into three classes (low, medium, and high). Poorer results were obtained with an enhanced

multiplicative scatter correction (EMSC) treatment. For HSI, better results were achieved when a logarithmic transformation was applied to the α-amylase values, but this gave poorer results for FTIR (R^2 0.82 vs. 0.74). The authors also reported that all the models applied tend to overestimate enzymatic activity at low values and underestimate it at high values, and in conclusion they suggested using SWIR for its better prediction and for the advantages of extracting spatial information from the hypercube.

The Hagberg Falling Number (HFN), the industrially accepted method for the measurement of sprout damage in wheat, has been recently used as the reference measurement for quantitative models built by HSI (44). 425 wheat batches were scanned as whole kernels. The samples included wheats without any previous treatment, and laboratory-treated samples to force pre-germination at increasing degrees. PLS regression models had calibration R^2 values from 0.40 (raw spectra) to 0.60 (second derivative pre-treated spectra). On a HFN range of 62–281 s, the RMSEC was 50.4 s and RMSEP = 62.7 s. The authors also tested the possibility of using classification models to discriminate sound kernels from those with high enzymatic activity (low HFN), using Linear Discriminant Analysis (LDA). Using 250 s as the threshold, the model had accuracy of 86.4%, while using 150 s the accuracy was 97.9%, thus showing very good performance to detect highly damaged kernels. Interestingly, the kernels did not exhibit any visual sign of sprouting, which makes this research promising for possible screening purposes.

Viability and germination activity is of paramount importance in barley used for malting, and the presence of pre-germinated grains is of industrial relevance due to their inability to germinate again in malting. The analysis of pre-germinated barley using HSI in the NIR region (900–1700 nm) was reported recently in an experiment involving the addition of water to barley kernels to understand the effect of pre-germination on kernel sprouting (45). A total of 840 kernels were imaged, sampled at eight times after soaking in water up to 60 h. After drying and storing the kernels in a refrigerator, the percentage of germinated kernels was evaluated by clustering them into three groups, i.e. normal, delayed and limited regermination. In addition, mathematical models were tested to predict the pre-germination time on a single kernel basis. The authors grouped the kernels into three soaking times, i.e. 0–18, 24—36, and 48–60 h and obtained a classification error of 32%, while it was 3% on bulk barley.

HSI was also used for estimation of cereal grain viability, i.e. assessing the germination of kernels under controlled conditions (46). Whole sorghum, barley, and wheat kernels from different varieties were used to obtain a total of 8 samples, from which 10 kernels of each were randomly taken for HSI scanning and for the tetrazolium test, used as the reference measurement of kernel viability. The kernels were incubated in Petri dishes in a wet environment for up to 72 h and then frozen at −80 °C, freeze-dried and analyzed by HSI in the range 1000–2500 nm. The region 1920–1940 nm was reported as associated with a loss of kernel viability. Partial Least Squares Discriminant Analysis (PLS-DA) was built to differentiate between viable and non-viable kernels, using single pixel data within the hypercube. However, the model was relatively poor, with above 26% of false positives. Furthermore, the approach of using freeze-dried kernels removes the benefit of HSI of rapid analysis, due to the long sample preparation required.

Other properties of cereal grains were assessed by NIR spectroscopy, in particular β-glucan in barley and malt (47), but no work on this compound by HSI has been published so far. Sá and Palmer (47) scanned 319 kernels in the range 900–1700 nm, reporting satisfactory prediction of β-glucan content in terms of repeatability and standard error of cross

validation (SECV = 0.15 mg/grain, on a range from 0 to 0.9 mg/grain). However, the correlation coefficient was low, i.e., $R^2 = 0.58$, which was attributed to the combined effect of kernel size, hardness, and protein content.

Schmidt et al. (48) tested different types of NIR instruments to predict β-glucan content in naked barley, using 107 barley samples, as whole grain or milled. Three acquisition modes were used: a transmission instrument working in the spectral range 850–1048 nm, an instrument working in reflectance mode in the region 400–2498 nm and a FT-NIR spectroscopy instrument acquiring spectra at 800–2780 nm. A PLS regression method was used for the calibration for β-glucan content, with R^2 ranging from 0.77 to 0.99, depending on the instrument used and whether the samples are whole or ground. The worst performance was obtained for Near Infrared Transmittance (NIT) on whole grains, while the best performance was reported for FT-NIR on ground meal. The values of SECV were between 0.15% and 0.47% (range = 3.3–7.4%), where the lowest value was obtained for FT-NIR on milled samples. It was also highlighted that useful information for β-glucan content can be obtained in the range 850–1050 nm, with the only important exception for black barley samples. This is of industrial relevance as detectors in this spectral range are less expensive than those working at longer wavelengths, e.g. 1000–2500 nm.

A similar work reported on β-glucan prediction in naked oats (49). The whole dataset comprised 168 naked oat samples from 12 varieties obtained from three harvest years, and scans were made both on whole grains and on flours. Transmission spectra were obtained in the range 800–1048 nm, while reflectance ones were taken from 400 to 2500 nm. A new regression strategy named partial robust M-regression (PMR), similar to PLS regression, was used for the prediction of β-glucan content. RMSEC and RMSEP for β-glucan were 0.22 and 0.28% for whole grains in transmission mode. In the case of flour, the results were slightly improved, whereas the lowest prediction error was obtained in reflectance mode, with RMSEC = 0.20 and RMSEP = 0.24%.

Calibrations for moisture, starch, β-glucan, protein, oil, and ash in barley were developed also using Fourier transform equipment (4 cm^{-1} resolution), and two dispersive instruments (8 nm and 10 nm bandpass) (50). The prediction equations ranged from $R^2 = 0.96$ for moisture to 0.79 for β-glucan, and were suggested to be of sufficient robustness for screening or classification of whole kernel barley, except for β-glucan. The advantage of using higher spectral resolution was only reported for starch content.

In addition to these properties, HSI has been usefully applied for the study of cereal seed coating. For example, NIR and HSI were applied for the assessment of homogeneity of pesticide coating on cereal seeds, which might be of interest for agriculture applications. HSI discrimination was carried out using PLS-DA, while quantitative models were built by PLS regression. The results showed that HSI had slightly poorer classification performances compared to NIR spectroscopy in discriminating the treated and non-treated kernels. The quantification model allowed defining two groups for the wheat kernels, i.e., underdose and overdose of pesticide coating (51).

5. NIR and HSI for rice quality control and chemical composition

NIRS has been proposed for evaluating rice quality during its processing, particularly for detecting moisture and protein content. A system NIR transmittance instrument scanning 33 wavelengths in the region 825–1075 nm was described by Kawamura et al. (52). Good performance

was obtained for automatic detection of average protein content, moisture content and sound whole kernel ratio. The accuracy for protein content prediction in whole brown rice was $R^2 = 0.70$ and SEP 0.24%. On milled rice, it was $R^2 = 0.76$, with a SEP of 0.22%.

Prediction of moisture content in rice was also reported by Lin et al. (53), who used HSI in the NIR region 870–1014 nm, with just 15 wavelengths. MLR, PLS regression and ANN were tested to predict moisture in bulk samples. The R^2 value for the best model had R^2 value of 0.952. The prediction error was between 0.435 and 0.479%, thus showing very good performance, almost comparable with traditional NIR spectrometers.

Discrimination of Basmati rice from other lower value varieties was reported by other researchers using NIR spectroscopy (54). Twenty-three single grains were taken from 116 samples, scanned in NIR transmittance mode (range 850–1050 nm) and the spectra of 62 bulk samples were used for calibration. Discriminant analysis was proved as more effective compared to PCA, enabling identification of all Basmati samples used. However, other rice samples were misclassified as Basmati with a cross-validation error rate from 8.2 to 20%. The authors suggested further investigations to establish whether the discrimination is satisfactory for a wider population of rice samples, as the authors used a limited number of Basmati rice.

Deng, Zhu and Huang (55) investigated an identification method for rice seed based on HSI technology in the range 400–1000 nm, using 700 rice kernels from 6 short grain varieties. A clustering algorithm using K-means classification was applied to build semi-supervised classifiers, and the highest accuracy obtained was 91.95%.

The issue related to rice adulteration was also addressed by studying the classification capacity of HSI for mixtures of high price rice cultivar (Chang-Li-Xiang) and a low quality one (Li-Shui), at different proportions (56). Hyperspectral images were acquired in the range 390–1050 nm, and the adulteration was established by using support vector machine (SVM) on the whole spectra for bulk samples. The cross-validation accuracy reached 93% and prediction accuracy was 98%. By selecting the six most characteristic wavelengths or the optimal number of PC, the prediction accuracy of the model was 96% and 98%, respectively.

Zhao (57) applied HSI for the detection of illegally waxed rice, i.e., rice with added industrial wax. Spectral were acquired from 80 waxed kernels and 80 non-waxed rice, in spectra range 400–1000 nm, using 100 grains for the calibration. PLS and linear discriminant analysis (LDA) were tested, and waxed rice was detected at a rate of 80% and 93.3%, respectively. Therefore, HSI seems to be a reliable method for waxed rice detection. Even higher classification accuracy was reported in a more recent work by the same research group, where the "successive projections algorithm" (SPA) was applied to select the most effective wavelengths for the prediction models, reaching 96% classification accuracy by LDA (58).

Sumriddetchkajorn et al. (59) tested the use of multispectral fluorescence imaging for Thai rice cultivar identification by applying two fluorescence wavelengths at 540 and 575 nm with UVC excitation at 265 nm. Milled rice grains from 8 Thai rice breeds were tested and the authors reported the feasibility of the proposed method to identify Thai rice breeds. However, no repeatability and reliability test was reported.

Rice bran was evaluated in another work on a single rice grain basis by using HSI in the spectral range 400–1000 nm. Before milling, rice samples were scanned by HSI and the ground rice was dyed to enable the identification of the residual bran, which was scanned again by HSI. A comparison between the HSI prediction model and the evaluation through optical microscopy analysis resulted in an estimation accuracy of 93.5%. Statistical

techniques such as PCA, SVM, and LDA were compared to verify the classification between grains with excessive residual bran and those with acceptable low bran content (60).

Other recent publications reported on the possible use of HSI to discriminate rice cultivars. Wang et al. (61) acquired hyperspectral images in the range 400–1000 nm for paddy rice samples, and information such as chalkiness degree and shape features were extracted and used for subsequent cultivar discrimination by PCA and back propagation neural network (BPNN). Both models were tested for their discrimination ability using the seven optimal wavelengths, reaching an accuracy of 89.2 and 89.9% for PCA and BPNN, respectively.

Kong et al. (2013) also studied classification of rice cultivars by applying a Random Forest (RF) classification algorithm from hyperspectral data in the NIR range 874–1734 nm. Approximately 50 kernels were analyzed for each of the four rice cultivars. The 12 optimal wavelengths were selected, and several statistical models were tested for their discrimination ability. Optimal wavelength selection gave an accuracy above 80%, whereas the best performances were obtained from full-spectra classification models, reaching 100% accuracy using SIMCA, SVM and Random Forest classification (62).

Among rice quality parameters, starch gelatinization properties are relevant because they are directly related to the cooking properties of rice, especially the cooking time, cooked rice hardness, and stickiness (63).

Sohn et al. (64) investigated the protein and amylose content in rice flour by applying NIR spectroscopy and testing several spectral pre-treatments including derivatives. Further studies applied NIR for the investigation of pasting properties and gel texture in rice (65).

Some calibrations based on NIRS to predict the gelling properties and generally the cooking characteristics of rice were reported to be satisfactory. On approximately 600 rice samples scanned, prediction of gel consistency had R^2 value of ~0.7, while the R^2 value for alkali spread score was higher than 0.81, and for amylose content it was above 0.93. The model had generally better performance for milled rice, while the best predictions were obtained for brown rice (66).

NIR spectroscopy was applied for the prediction of protein and amylase content in rice flour (67). The authors scanned the samples in the range 424–2498 nm at 8 nm intervals. Protein content in brown flour samples was predicted with $R^2 = 0.943$ and SEC = 0.301%. The best results from the cross-validation were $R^2 = 0.941$ and SEC = 0.308%. Amylose content was predicted with slightly less accuracy, with the best R^2 for brown rice flour being 0.757 and SEC = 1.760%. The cross-validation set gave $R^2 = 0.729$ and SECV = 1.928%. The milled flour samples always resulted in poorer calibration performances than the brown rice flour (67). In a further work by the authors, in which they reported the prediction of gelatinization and pasting properties of milled rice flours, NIRS calibrations were built from 300 Indica rice lines. The milled rice was scanned in the range 1100–2500 nm, while several models were built from parameters obtained by Differential Scanning Calorimetry (DSC), Rapid Visco Analyser (RVA) and alkali spreading value (ASV). Several properties were poorly predicted, while pasting temperature by RVA had good $R^2 = 0.858$ and RPD values above 4 (68).

6. Application of NIR and HSI for maize kernel evaluation

Hyperspectral imaging technology has been recently applied for maize analysis by several authors. Cogdill et al. (69) analyzed single kernel maize by NIR spectroscopy in transmittance mode in the region 750–1090 nm. Moisture and oil content were predicted using PLS

and principal component regression (PCR). Calibration using a total of 473 kernels gave a SEC and SECV of 1.05% and 1.20% for moisture, and 1.09% and 1.38% for oil, respectively. Results for oil were poorer than expected, and much of the error was attributed to the reference method used for oil determination. However, the performance was considered satisfactory for use of this technique at practical level, after further refinements.

Weinstock et al. (70) used microscopic near-infrared (NIR) reflectance hyperspectral imaging in the region 950–1700 nm to discriminate the kernel germ from the endosperm region. A PLS calibration was developed for 200 maize kernels to predict the oil and oleic acid concentrations. The RMSEP values were 0.7% for oil content and very high, 14%, for oleic acid prediction.

A recent paper reported the use of HSI for variety discrimination of maize kernels between waxy and sweet maize (71). The authors acquired the hypercubes in the region 400–1000 nm from 270 maize kernels as the calibration set, with a further 108 kernels used as the test set. Six optimal spectral wavelengths were selected to apply a least-square support vector machine (LS-SVM) classification model. The model based on the full spectra gave 93.3% calibration accuracy and 90.7% prediction accuracy, while the model based on the best 6 wavelengths had an accuracy of 91.1% and 87.0% for calibration and prediction, respectively.

Zhou et al. (72) studied maize by-products by NIR spectroscopy in the full NIR region (1000–2500 nm), by focusing on the so-called corn distillers' dried grains with solubles (DDGS) to verify the possibility of classifying their geographical origin. PLS discriminant analysis gave promising results in discriminating the four different geographical regions, i.e., Europe, USA, and two locations of China.

Nansen et al. (73) reported that maize grinding influences HSI classification accuracy of two near-isogenic inbreed maize lines, using the spectral range 435–769 nm. Sample presentation greatly influenced classification ability, with R^2 value improving from 0.141 in whole kernels to 0.529 for finely ground material. The classification error was almost three times lower for finely ground maize than that of whole kernels.

Maize kernel hardness has also been studied by NIR or HSI (74). The researchers published a study of maize kernels using HSI to discriminate between hard, intermediate and soft maize kernels from inbred lines. Samples were scanned in the range 960–1662 nm and 1000–2498 using two spectral imagers. PLS-DA models were constructed and applied at single pixel level to discriminate between glassy and floury kernels, from three batches belonging to a hard, medium, and soft class. Using the PLS-DA model, maize hardness was deduced from the ratio between glassy and floury endosperm of the kernels, but no reference method was used to assess the actual hardness of the wheat samples. The results were promising, with $R^2 = 0.76$, but only 12–24 kernels were used and thus a larger number of samples are needed in future works for a more robust evaluation and independent validation, also using appropriate reference measurements (18). A similar work reported a coefficient of determination of 85% for maize hardness, using PLS-DA classification (75).

7. Study of mycotoxins and fungal attacks on cereal grains by NIR and HSI

Maize mycotoxins are a common problem in every producing country, and toxigenic fungal growth can dramatically affect the quality and safety of the products, both for human and

animal nutrition. Traditional NIR spectroscopy has been used in several applications for the detection of mycotoxigenic fungi and their toxic metabolites. Hence, Berardo et al. (76) evaluated 208 maize samples from 16 areas of Italy, after artificial inoculation with *Fusarium verticilloides* and the concentrations of their metabolites were quantified by reference methods. Samples were scanned as whole kernels or ground in the spectral range 400–2500 nm. PLS regression was used to predict the incidence of kernels infected by fungi. Total fungal infection was predicted with better accuracy in kernels compared to meals, with $R^2 = 0.79$ and SECV = 9.40 mg kg^{-1}, vs. $R^2 = 0.66$ and SECV = 5.91 mg kg^{-1}. Separate models were built for the rate of fungal infection, *F. verticilloides* infection and concentration of ergosterol and fumonisin B_1. The SEP was 6.34% (range = 65–100%) total fungal infection, and 9.64% (range = 30–100%) for *F. verticilloides* infection. For ergosterol and fumonisin B_1, the SEP was 1.74 (range = 0–18) and 1.33 mg kg^{-1} (range = 0–12). It was therefore suggested that NIR could be a useful alternative to expensive and time-consuming HPLC analysis of fungal toxins. In particular, the authors propose the use of NIR to monitor mould contamination in postharvest maize to differentiate contaminated from clean grain (76).

Williams et al. (77) inoculated maize kernels with *F. verticilloides*, and then scanned the samples by hyperspectral imaging in the NIR region 1000–2500 nm. Images were taken at nine times up to 90 h from incubation, by averaging the spectra of several kernels placed on Petri dishes. The main variability was found in the spectral range 1900–2136 nm, where the chemical information is mainly related to protein, water and starch content. The PLS regression models to predict time after inoculation gave a prediction ability (R^2) of 0.83–0.98, and a RMSEC from 7.0 to 14.6 h, depending on kernel sterilization and position (crease-down and crease-up).

NIR spectroscopy was also used to sort sound batches of wheat downgraded for fungal contamination due to *Fusarium* (78). A BoMill TriQ sorter was used for soft or hard wheat and barley, by applying existing calibrations for crude protein content and mycotoxin level for single grains. No data were reported on the calibration itself, as this is a proprietary protocol. The system acquired NIR spectra (1100–1700 nm) in transmittance mode and the sorting machine produced ten fractions, which were analyzed to assess fungal attack (*Fusarium*), deoxynivalenol, crude protein, thousand kernel weight and bushel weight. The statistical correlations based on Pearson coefficients were reported among the ten fractions. It was suggested to use the crude protein value as an indirect indication of *Fusarium* attack, as the latter is positively correlated with deoxynivalenol ($r = 0.90$) and negatively correlated with protein content, with $r = -0.27$.

A similar experiment using HSI was reported on maize inoculated with *Aspergillus flavus*. From two commercial hybrids, a total of 60 kernels were sampled for scanning in the spectral region 1000–2500 nm. The first two PCs from single pixel data were suggested to be associated with infected and healthy maize kernels, respectively, while PC_3–PC_5 mainly showed textural characteristics. The wavelengths at 1729 and 2344 nm were identified as strongly correlated with Aflatoxin B1, from the PC loading plot. HSI was evaluated as satisfactory for clustering maize kernels into different levels of fungal attacks, with classification accuracy of 92.3% (79).

HSI was also used to evaluate the level of mildew growth in soft red winter wheat kernels. Shahin et al. (80) applied HSI in the range 400–1000 nm to predict mildew damage in Canadian wheats. Wheats were visually classified into 9 classes, and PLS regression was used to predict the incidence of mildew damage. R^2 and RMSE on the calibration set were 0.869 and

0.75, respectively. The prediction accuracy into the nine classes was approximately 91%. Shahin et al. (81) studied two spectral regions by HSI, 400–1000 and 1000–2500 nm, for the same purpose. Two sets of samples were used, comprising 68 (calibration) samples from the 2008 harvest and 27 (validation) from 2009. PLS regression models were built against 9 classes of mildew damage level. Mildew damage affected mainly the intensity and slope changes in the 450–950 nm spectral range. For the second spectral range tested, the main differences due to mildew damage were recorded between 1000 and 2000 nm. The best PLS regression model was obtained for the first region (450–950 nm) and has a RMSE of 1.19 for the test set, whereas it was not associated with any specific wavelength. This was attributed to maize discoloration due to fungal attack. For practical purposes, misclassification in an adjacent class is however acceptable, and therefore the outcomes might have practical interest.

The same authors also used visible-NIR hyperspectral imaging for the detection of *Fusarium* damage in Canadian wheat samples (82). A set of 5,221 individual kernels of seven major classes of Canadian wheat were scanned in the spectral region 400–1000 nm. A PLS-DA model was built to discriminate sound or damaged kernels. PLS to predict the score of *Fusarium* damaged kernels had quite poor performance, with $R^2 = 0.52–0.62$ for the calibration, and RMSECV = 0.30–0.34. Reducing the number of bands to three wavelengths resulted in poorer models. Nevertheless, the calibration performance was not much lower, with interesting consequences in terms of industrial applicability of multispectral systems. The classification accuracy for single kernels from a PLS-DA model based on four wavelengths (494, 578, 639, and 678 nm) was approximately 90% for the overall samples (for both calibration and validation sets). In case of severely damaged kernels, the accuracy was very high (99%). However, it should be noted that reference classification was done by visual classification of the kernels into sound, mild damage and severe damage.

Attempts to apply HSI to maize kernels artificially inoculated by different fungal species, *A. niger, F. graminearum, A. flavus* and *A. parasiticus*, were reported by Del Fiore et al. (83). Twelve commercial maize hybrids were tested, each with three groups created by conditioning the kernels at 15, 20, and 30% humidity. The spectral region considered was between 400 and 1000 nm, and no spectral treatment was applied, except reflectance calculation and white and black removal. A PCA followed by Discriminant Analysis was used to assess whether sound kernels were different from those at different times after inoculation, from 1 day to 7 days. A statistically significant difference was observed from kernels contaminated for 48 h, which was sufficient to cause changes in the spectra due to the fungal activity. This discrimination was carried out using three selected wavelengths for *A. flavus* (410, 535, and 945 nm). In the case of *A. niger*, the authors noted that contamination causes an increase in absorbance in the visible region, but a decrease in the NIR range. The discrimination was possible after 4 days from inoculation, while it was unsuccessful for other fungi.

The rate of fungal infection was also assessed in rice by traditional NIR spectroscopy, using both naturally-contaminated samples and a second group artificially inoculated by *Aspergillus spp* (84). Jasmine rice, white rice, and brown rice samples were used as sound, for a total of 90 batches, and another 16 samples were artificially inoculated. The direct planting method was used as the reference method to assess fungal contamination. Diffuse NIR spectroscopy was used in the spectral range 950–1650 nm. The PLS model to predict total fungal infection demonstrated that the best performance was achieved on the raw reflectance data with no spectral pre-treatment, with validation $R^2 = 0.688$ and SEP = 28.9% (range 1–100%), using 222 samples for the calibration. The prediction of rice infected by *Aspergillus* was poorer, and the best

model was obtained using the maximum normalization pre-treatment, with validation $R^2 = 0.437$ and SEP = 18.7% for the validation set. It should be also noted that the samples artificially infected by *Aspergillus* were not uniformly distributed, as the majority of kernels had infection rate close to zero, with very few kernels in the top range.

For an overview on the use of HSI for determination of other biological contaminants in food products please refer to Vejarano et al. (85).

8. Other applications of NIR and HSI in cereal grains

Water uptake is of interest for farmers and agronomists, as well as from the processing industry. Alternative methods have been applied for the study of seed imbibition, e.g., magnetic resonance micro-imaging, but the equipment required is still expensive, thus NIRS-based methods can offer better insights into the water uptake process in a non-destructive and rapid way (86). Wheat conditioning, i.e., addition of water before milling, is a paramount step in flour milling production, for this reason some studies focused on the use of HSI to visualize water uptake in seeds and grains. Manley, Du Toit and Geladi (87) investigated water uptake in six wheat cultivars divided into three hardness categories (soft, hard, and very hard) using HSI in the range 1000–2498 nm. Six conditioning times were used, up to 36 h to reach a final water content of 17%, considering the initial moisture levels. The spectra were analyzed by PCA, and the authors reported that PC1 explained kernel curvature, possibly combined with some effect of surface moisture. The authors claimed that visualization of water uptake was possible from PC3, for which the loading plot showed a prominent absorption at ~1940 nm. It was also suggested that discrimination between free and bound water is possible by measuring the absorption at 1910 nm, indicating free water, and the absorption at 1940 nm, related to bound water in the kernel. In addition, the authors hypothesized that water absorbed by wheat grains during conditioning is present as bound water in the kernels. An attempt using deuterated water was reported to better track water diffusion, but the effect of deuterium diffusion was very weak compared to distilled water.

Lancelot et al. (88) recently applied HSI for the study of kinetics of water uptake in wheat kernels. The authors cut the wheat kernels by placing the part containing the embryo in a sample holder, so they were able to scan the cut surface at different water exposure times (0, 30 min, 1 h, 5 h, 9 h, 24 h, 28 h, 33 h). A push-broom system detecting the NIR spectrum in the range 950–2500 nm was used, PCA and non-negative least squares algorithm (NNLS) were used for the chemometrics. The five seeds analyzed had different water uptake kinetics, and the loadings showed that bands at 1450 and 1940 nm were the most affected.

Heat damage in wheat causes protein denaturation and reduces processing quality. Heat-damaged wheat was evaluated at single kernel level using reflectance NIR in the region 400–1700 nm in hard red spring and hard white wheats (89). 300 grams of each class were conditioned at 17% moisture and dried to create heat damage. 520 kernels for each class were used, but they were not fully independent samples. The visible region was less accurate in detecting heat damage, while the remaining region gave 100% prediction accuracy by PLS regression. The prediction was mainly based on differences in the light scattering.

Whereas this review is not focused on processed food, there are examples of HSI applied to cereal products used as feed, also in complex mixtures. For instance, Fernández-Pierna, Baeten and Dardenne (90) applied a method for rapid screening of compound feeds by HSI in the NIR region 900–1700 nm. 13 different vegetal ingredients were evaluated in mixture:

barley, coconut, corn, flax, lucerne, manioc, palm, rapeseed, soya bean, sugar beet, sunflower, sweet peas, and wheat. A classification tree was constructed to sort the 13 species in a dichotomist way, and Support Vector Machines (SVM) was used to construct the discrimination model. The model had an accuracy of 99–100% for the calibration set and reached 95.3% for the test set, which suggests its use at the industrial level for rapid screening purposes.

9. Conclusions

This review has reported on the recent scientific literature about the applications of near-infrared spectroscopy and hyperspectral imaging for the evaluation of cereal grains. HSI has been shown to be a versatile tool for the study of cereal grains allowing a rapid analysis at single kernel basis. One of the main advantages is the possibility of assessing 100% of the grains individually, instead of taking average data for the batch, and this in turn could be useful for better understanding plant physiology, natural single-kernel variability, and the mechanisms involved in the germination process. The other obvious benefit in using HSI is the possibility of multi-component analysis, e.g., quantification of moisture and protein content, as well as other minor compounds or more complex properties, for example, predicting the rheological behavior of dough or bread by imaging wheat grains. The accuracy of the prediction models and the need for efficient methods of data handling are important factors to consider when applying NIR-based instruments and in particular HSI, especially when implementing this technology for practical applications. HSI represents one of the most promising non-contact technologies able to give rapid chemical information and provide insight into the spatial distribution of chemical properties. Thus, wider applications of HSI at the food industry level and for research purposes, e.g., in breeding programmes, are expected.

Acknowledgments

This work was supported by the Biotechnology and Biological Sciences Research Council [grant number BB/N021126/1]. François Chenevarin is acknowledged for the manuscript proofreading.

Funding

Biotechnology and Biological Sciences Research Council (BB/N021126/1).

References

1. Osborne, B. G., Fearn, T., and Hindle, P. H. (1993) Practical NIR spectroscopy with applications in food and beverage analysis. *Longman Sci. Tech*. Harlow, UK, p. 227. ISBN : 0582099463.
2. Gowen, A., O'Donnell, C., Cullen, P., Downey, G., and Frias, J. (2007) Hyperspectral imaging—An emerging process analytical tool for food quality and safety control. *Trends Food Sci. Tech.* 18: 590–598.
3. Elmasry, G., Kamruzzaman, M., Sun, D.-W., and Allen, P. (2012) Principles and applications of hyperspectral imaging in quality evaluation of agro-food products: A review. *Crit. Rev. Food Sci. Nutr.* 52: 999–1023.

4. Wu, D., and Sun, D.-W. (2013) Advanced applications of hyperspectral imaging technology for food quality and safety analysis and assessment: A review—Part I: Fundamentals. *Innovative Food Sci. Emerg. Technol.* 19: 1–14.
5. Huang, H., Liu, L., and Ngadi, M. O. (2014) Recent developments in hyperspectral imaging for assessment of food quality and safety. *Sensors* 14: 7248–7276.
6. Vidal, M., and Amigo, J. M. (2012) Pre-processing of hyperspectral images. Essential steps before image analysis. *Chemom. Intell. Lab. Syst.* 117: 138–148.
7. Feng, Y.-Z., and Sun, D.-W. (2012) Application of hyperspectral imaging in food safety inspection and control: A review. *Crit. Rev. food Sci. Nutr.* 52: 1039–1058.
8. Lorente, D., Aleixos, N., Gómez-Sanchis, J., Cubero, S., García-Navarrete, O. L., and Blasco, J. (2012) Recent advances and applications of hyperspectral imaging for fruit and vegetable quality assessment. *Food Bioprocess Tech.* 5: 1121–1142.
9. Ferrari, C., Foca, G., and Ulrici, A. (2013) Handling large datasets of hyperspectral images: Reducing data size without loss of useful information. *Anal. Chim. Acta* 802: 29–39.
10. Raychaudhuri, B. (2016) Imaging spectroscopy: Origin and future trends. *Appl. Spectrosc. Rev.* 51: 23–35.
11. Norris, K., (1982) Use of Near-Infrared Reflectance Spectroscopy and Dye-binding techniques for estimating protein in oat groats. *Cereal Chem.* 59: 333–335.
12. Downey, G., and Byrne, S. (1983) Determination of protein and moisture in ground wheat by near infra-red reflectance spectroscopy. *Irish J. Food Sci. Tech.* 135–146.
13. Williams, P. C., Stevenson, S. G., Starkey, P. M., and Hawtin, G. C. (1978) The application of near-infrared reflectance spectroscopy to protein−testing in pulse breeding programmes. *J. Sci. Food Agric.* 29: 285–292.
14. Williams, P. C., and Sobering, D. (1993) Comparison of commercial near infrared transmittance and reflectance instruments for analysis of whole grains and seeds. *J. Near Infrared Spectro.* 1: 25–32.
15. Ozaki, Y., McClure, W. F., and Christy, A. A. (2006) *Near-infrared spectroscopy in food science and technology*. New York: John Wiley & Sons.
16. Delwiche (1995) Single wheat kernel analysis by near-infrared transmittance: Protein content. *Cereal Chem.* 72: 11–16.
17. Nielsen, J. P., Pedersen, D. K., and Munck, L. (2003) Development of nondestructive screening methods for single kernel characterization of wheat. *Cereal Chem.* 80: 274–280.
18. Williams, P., Geladi, P., Fox, G., and Manley, M. (2009) Maize kernel hardness classification by near-infrared (NIR) hyperspectral imaging and multivariate data analysis. *Anal. Chim. Acta* 653: 121–130.
19. Delwiche, S. R. (1998) Protein content of single kernels of wheat by near-infrared reflectance spectroscopy. *J. Cereal Sci.* 27: 241–254.
20. Delwiche, S., and Hruschka, W. (2000) Protein content of bulk wheat from near-infrared reflectance of individual kernels. *Cereal Chem.* 77: 86–88.
21. Halsey, S. A. (1987) Analysis of whole barley kernels using near-infrared reflectance spectroscopy. *J. Inst. Brew.* 93: 461–464.
22. Fox, G., Onley−Watson, K., and Osman, A. (2002) Multiple linear regression calibrations for barley and malt protein based on the spectra of hordein. *J. Inst. Brew.* 108: 155–159.
23. Fox, G., Kelly, A., Sweeney, N., and Hocroft, D. (2011) Development of a single kernel NIR barley protein calibration and assessment of variation in protein on grain quality. *J. Inst. Brew.* 117: 582–586.
24. Tarr, A., Diepeveen, D., and Appels, R. (2012) Spectroscopic and chemical fingerprints in malted barley. *J. Cereal Sci.* 56: 268–275.
25. Han, Z., Cai, S., Zhang, X., Qian, Q., Huang, Y., Dai, F., and Zhang, G. (2017) Development of predictive models for total phenolics and free *p*-coumaric acid contents in barley grain by near-infrared spectroscopy. *Food Chem.* 227: 342–348.
26. Fontaine, J., Schirmer, B., and Hörr, J. (2002) Near-infrared reflectance spectroscopy (NIRS) enables the fast and accurate prediction of essential amino acid contents. 2. Results for wheat, barley, corn, triticale, wheat bran/middlings, rice bran, and sorghum. *J. Agric. Food Chem.* 50: 3902–3911.

27. Manley, M., McGoverin, C. M., Snyders, F., Muller, N., Botes, W. C., and Fox, G. P. (2013) Prediction of triticale grain quality properties, based on both chemical and indirectly measured reference methods, using near-infrared spectroscopy. *Cereal Chem.* 90: 540–545.
28. Igne, B., Gibson, L., Rippke, G., Schwarte, A., and Hurburgh, C. (2007) Triticale moisture and protein content prediction by near-infrared spectroscopy (NIRS). *Cereal Chem.* 84: 328–330.
29. Serranti, S., Cesare, D., Marini, F., and Bonifazi, G. (2013) Classification of oat and groat kernels using NIR hyperspectral imaging. *Talanta* 103: 276–284.
30. Manley, M., McGoverin, C. M., Engelbrecht, P., and Geladi, P. (2012) Influence of grain topography on near-infrared hyperspectral images. *Talanta* 89: 223–230.
31. Pedersen, D. K., Martens, H., Nielsen, J. P., and Engelsen, S. B. (2002) Near-infrared absorption and scattering separated by extended inverted signal correction (EISC): Analysis of near-infrared transmittance spectra of single wheat seeds. *Appl. Spectrosc.* 56: 1206–1214.
32. Rinnan, Å., van den Berg, F., and Engelsen, S. B. (2009) Review of the most common pre-processing techniques for near-infrared spectra. *Trends Anal. Chem.* 28: 1201–1222.
33. Ravikanth, L., Singh, C. B., Jayas, D. S., and White, N. D. (2015) Classification of contaminants from wheat using near-infrared hyperspectral imaging. *Biosystems Eng.* 135: 73–86.
34. Mahesh, S., Manickavasagan, A., Jayas, D., Paliwal, J., and White, N. (2008) Feasibility of near-infrared hyperspectral imaging to differentiate Canadian wheat classes. *Biosystems Eng.* 101: 50–57.
35. Gorretta, N., Roger, J., Aubert, M., Bellon-Maurel, V., Campan, F., and Roumet, P. (2006) Determining vitreousness of durum wheat kernels using near-infrared hyperspectral imaging. *J. Near Infrared Spectro.* 14: 231.
36. Shahin, M. A., and Symons, S. J. (2008) Detection of hard vitreous and starchy kernels in amber durum wheat samples using hyperspectral imaging (GRL Number M306). *NIR News* 19: 16–18.
37. Caporaso, N., Whitworth, M. B., and Fisk, I. D. (2017) Protein content prediction in single wheat kernels using hyperspectral imaging. *Food Chem.* 240: 32–42.
38. Mares, D., and Mrva, K. (2014) Wheat grain preharvest sprouting and late maturity alpha-amylase. *Planta* 240: 1167–1178.
39. Shafqat, S. (2013) *Effect of different sprouting conditions on alpha amylase activity, functional properties of wheat flour and on shelf-life of bread supplemented with sprouted wheat.* in, University of Guelph, Guelph, Ontario, Canada, p. 120.
40. Koç, H., Smail, V. W., and Wetzel, D. L. (2008) Reliability of InGaAs focal plane array imaging of wheat germination at early stages. *J. Cereal Sci.* 48: 394–400.
41. Xing, J., Van Hung, P., Symons, S., Shahin, M., and Hatcher, D. (2009) Using a short wavelength infrared (SWIR) hyperspectral imaging system to predict alpha amylase activity in individual Canadian western wheat kernels. *Sensing Instrum. Food Qual. Saf.* 3: 211–218.
42. Xing, J., Symons, S., Shahin, M., and Hatcher, D. (2010) Detection of sprout damage in Canada Western Red Spring wheat with multiple wavebands using visible/near-infrared hyperspectral imaging. *Biosystems Eng.* 106: 188–194.
43. Xing, J., Symons, S., Hatcher, D., and Shahin, M. (2011) Comparison of short-wavelength infrared (SWIR) hyperspectral imaging system with an FT-NIR spectrophotometer for predicting alpha-amylase activities in individual Canadian Western Red Spring (CWRS) wheat kernels. *Biosystems Eng.* 108: 303–310.
44. Caporaso, N., Whitworth, M. B., and Fisk, I. D. (2017) Application of calibrations to hyperspectral images of food grains: Example for wheat falling number. *J. Spectral Imaging* 6: 1–15.
45. Arngren, M., Hansen, P. W., Eriksen, B., Larsen, J., and Larsen, R. (2011) Analysis of pregerminated barley using hyperspectral image analysis. *J. Agric. Food Chem.* 59: 11385–11394.
46. McGoverin, C. M., Engelbrecht, P., Geladi, P., and Manley, M. (2011) Characterisation of non-viable whole barley, wheat and sorghum grains using near-infrared hyperspectral data and chemometrics. *Anal. Bioanalytical Chem.* 401: 2283–2289.
47. Sá, R. M., and Palmer, G. (2006) Analysis of $\beta-$Glucan in single grains of barley and malt using NIR−spectroscopy. *J. Inst. Brew.* 112: 9–16.
48. Schmidt, J., Gergely, S., Schönlechner, R., Grausgruber, H., Tömösközi, S., Salgó, A., and Berghofer, E. (2009) Comparison of different types of NIR instruments in ability to measure β-glucan content in naked barley. *Cereal Chem.* 86: 398–404.

49. Bellato, S., Frate, V. D., Redaelli, R., Sgrulletta, D., Bucci, R., Magrì, A. D., and Marini, F. (2011) Use of near infrared reflectance and transmittance coupled to robust calibration for the evaluation of nutritional value in naked oats. *J. Agric. Food Chem.* 59: 4349–4360.
50. Sohn, M., Himmelsbach, D. S., Barton, F. E., Griffey, C. A., Brooks, W., and Hicks, K. B. (2008) Near-infrared analysis of whole kernel barley: Comparison of three spectrometers. *Appl. Spectrosc.* 62: 427–432.
51. Vermeulen, P., Flémal, P., Pigeon, O., Dardenne, P., Fernández Pierna, J., and Baeten, V. (2017) Assessment of pesticide coating on cereal seeds by near infrared hyperspectral imaging. *J. Spectral Imaging* 6: 1–7.
52. Kawamura, S., Natsuga, M., Takekura, K., and Itoh, K. (2003) Development of an automatic rice: Quality inspection system. *Comput. Electron. Agric.* 40: 115–126.
53. Lin, L.-H., Lu, F.-M., and Chang, Y.-C. (2006) Development of a near-infrared imaging system for determination of rice moisture. *Cereal Chem.* 83: 498–504.
54. Osborne, B., Mertens, B., Thompson, M., and Fearn, T. (1993) The authentication of Basmati rice using near infrared spectroscopy. *J. Near Infrared Spectro.* 1: 77–83.
55. Deng, X., Zhu, Q., and Huang, M. Semi-supervised classification of rice seed based on hyperspectral imaging technology. *Am. Soc. Agric. Biolo. Eng.* 141912601.
56. Sun, J., Jin, X., Mao, H., Wu, X., and Yang, N. (2014) Application of hyperspectral imaging technology for detecting adulterate rice. *Trans. Chin. Soc. Agric. Eng.* 30: 301–307.
57. Zhao, M. (2014) Hyperspectral visible-near infrared imaging for the detection of waxed rice, in: SPIE/COS Photonics Asia. *Int. Soc. Opt. Photonics* 927622-927622-927613.
58. Li, B., Zhao, M., Zhou, Y., Hou, B., and Zhang, D. (2016) Detection of waxed rice using Visible-near infrared hyperspectral imaging. *J. Food Nutr. Res.* 4: 267–275.
59. Sumriddetchkajorn, S., Suwansukho, K., and Buranasiri, P. (2010) Two-wavelength spectral imaging-based Thai rice breed identification, in: SPIE Photonics Europe. *Int. Soc. Opt. Photonics* 77150I-77150I-77110.
60. Chen, W.-T., and Kuo, Y.-F. (2014) Observation and measurement of residual bran on milled rice using hyperspectral imaging. *Cereal Chem.* 91: 566–571.
61. Wang, L., Liu, D., Pu, H., Sun, D.-W., Gao, W., and Xiong, Z. (2015) Use of hyperspectral imaging to discriminate the variety and quality of rice. *Food Anal. Methods* 8: 515–523.
62. Kong, W., Zhang, C., Liu, F., Nie, P., and He, Y. (2013) Rice seed cultivar identification using near-infrared hyperspectral imaging and multivariate data analysis. *Sensors* 13: 8916–8927.
63. Juliano, B. O., and Perez, C. M. (1983) Major factors affecting cooked milled rice hardness and cooking time. *J. Texture Stud.* 14: 235–243.
64. Sohn, M., Barton, F. E., McClung, A. M., and Champagne, E. T. (2004) Near-infrared spectroscopy for determination of protein and amylose in rice flour through use of derivatives. *Cereal Chem.* 81: 341–344.
65. Bao, J., Shen, Y., and Jin, L. (2007) Determination of thermal and retrogradation properties of rice starch using near-infrared spectroscopy. *J. Cereal Sci.* 46: 75–81.
66. Wu, J., and Shi, C. (2007) Calibration model optimization for rice cooking characteristics by near infrared reflectance spectroscopy (NIRS). *Food Chem.* 103: 1054–1061.
67. Xie, L., Tang, S., Chen, N., Luo, J., Jiao, G., Shao, G., Wei, X., and Hu, P. (2014) Optimisation of near-infrared reflectance model in measuring protein and amylose content of rice flour. *Food Chem.* 142: 92–100.
68. Xie, L., He, X., Duan, B., Tang, S., Luo, J., Jiao, G., Shao, G., Wei, X., Sheng, Z., and Hu, P. (2015) Optimization of Near-infrared reflectance model in measuring gelatinization characteristics of rice flour with a rapid viscosity analyzer (RVA) and differential scanning calorimeter (DSC). *Cereal Chem.* 92: 522–528.
69. Cogdill, R. P., Hurburgh, C., Rippke, G. R., Bajic, S. J., Jones, R. W., McClelland, J. F., Jensen, T. C., and Liu, J. (2001) *Single-kernel maize analysis by near-infrared hyperspectral imaging*. Iowa: Iowa State University.
70. Weinstock, B. A., Janni, J., Hagen, L., and Wright, S. (2006) Prediction of oil and oleic acid concentrations in individual corn (*Zea mays* L.) kernels using near-infrared reflectance hyperspectral imaging and multivariate analysis. *Appl. Spectrosc.* 60: 9–16.

71. Wang, L., Sun, D.-W., Pu, H., and Zhu, Z. (2015) Application of hyperspectral imaging to discriminate the variety of maize seeds. *Food Anal. Methods*. 9: 225–234.
72. Zhou, X., Yang, Z., Haughey, S. A., Galvin-King, P., Han, L., and Elliott, C. T. (2014) Classification the geographical origin of corn distillers' dried grains with solubles by near infrared reflectance spectroscopy combined with chemometrics: A feasibility study. *Food Chem.* 189: 13–18.
73. Nansen, C., Kolomiets, M., and Gao, X. (2008) Considerations regarding the use of hyperspectral imaging data in classifications of food products, exemplified by analysis of maize kernels. *J. Agric. Food Chem.* 56: 2933–2938.
74. Fox, G., and Manley, M. (2009) Hardness methods for testing maize kernels. *J. Agric. Food Chem.* 57: 5647–5657.
75. Manley, M., Williams, P., Nilsson, D., and Geladi, P. (2009) Near infrared hyperspectral imaging for the evaluation of endosperm texture in whole yellow maize (*Zea maize* L.) kernels. *J. Agric. Food Chem.* 57: 8761–8769.
76. Berardo, N., Pisacane, V., Battilani, P., Scandolara, A., Pietri, A., and Marocco, A. (2005) Rapid detection of kernel rots and mycotoxins in maize by near-infrared reflectance spectroscopy. *J. Agric. Food Chem.* 53: 8128–8134.
77. Williams, P., Geladi, P., Britz, T., and Manley, M. (2012) Investigation of fungal development in maize kernels using NIR hyperspectral imaging and multivariate data analysis. *J. Cereal Sci.* 55: 272–278.
78. Kautzman, M. E., Wickstrom, M. L., and Scott, T. A. (2015) The use of near infrared transmittance kernel sorting technology to salvage high quality grain from grain downgraded due to Fusarium damage. *Anim. Nutr.* 1: 41–46.
79. Wang, W., Lawrence, K., Ni, X., Yoon, S.-C., Heitschmidt, G., and Feldner, P. (2015) Near-infrared hyperspectral imaging for detecting Aflatoxin B 1 of maize kernels. *Food Control* 51: 347–355.
80. Shahin, M. A., Hatcher, D. W., and Symons, S. J. (2010) Assessment of mildew levels in wheat samples based on spectral characteristics of bulk grains. *Qual. Assur. Saf. Crops Foods* 2: 133–140.
81. Shahin, M. A., Symons, S. J., and Hatcher, D. W. (2014) Quantification of mildew damage in soft red winter wheat based on spectral characteristics of bulk samples: A comparison of visible-near-infrared imaging and near-infrared spectroscopy. *Food Bioprocess Tech.* 7: 224–234.
82. Shahin, M. A., and Symons, S. J. (2012) Detection of fusarium damage in Canadian wheat using visible/near-infrared hyperspectral imaging. *J. Food Meas. Char.* 6: 3–11.
83. Del Fiore, A., Reverberi, M., Ricelli, A., Pinzari, F., Serranti, S., Fabbri, A., Bonifazi, G., and Fanelli, C. (2010) Early detection of toxigenic fungi on maize by hyperspectral imaging analysis. *Int. J. Food Microbiol.* 144: 64–71.
84. Sirisomboon, C. D., Putthang, R., and Sirisomboon, P. (2013) Application of near infrared spectroscopy to detect aflatoxigenic fungal contamination in rice. *Food Control* 33: 207–214.
85. Vejarano, R., Siche, R., and Tesfaye, W. (2017) Evaluation of biological contaminants in foods by hyperspectral imaging (HSI): A review. *Int. J. Food Prop.*
86. Cozzolino, D., Degner, S., and Eglinton, J. (2015) In situ study of water uptake by the seeds, endosperm and husk of barley using infrared spectroscopy. *Spectrochim. Acta Part A: Mol. Biomol. Spectrosc.*
87. Manley, M., Du Toit, G., and Geladi, P. (2011) Tracking diffusion of conditioning water in single wheat kernels of different hardnesses by near infrared hyperspectral imaging. *Anal. Chim. Acta* 686: 64–75.
88. Lancelot, E., Bertrand, D., Hanafi, M., and Jaillais, B. (2017) Near-infrared hyperspectral imaging for following imbibition of single wheat kernel sections. *Vib. Spectrosc.* 92: 46–53.
89. Wang, D., Dowell, F., and Chung, D. (2001) Assessment of Heat-damaged wheat kernels using near-infrared spectroscopy. 1. *Cereal Chem.* 78: 625–628.
90. Pierna, J. F., Baeten, V., and Dardenne, P. (2006) Screening of compound feeds using NIR hyperspectral data. *Chemometrics and Intelligent Laboratory Systems* 84: 114–118.